Tensor Field Visualization with PDE's and Application to DT-MRI Fiber Visualization

David Tschumperlé Rachid Deriche

INRIA Sophia-Antipolis, Odyssée Lab
2004 Rte des Lucioles, BP93, 06902 Sophia-Antipolis, France
e-mail: {David.Tschumperle,Rachid.Deriche}@sophia.inria.fr

Abstract

We propose a PDE-based method to create textured representations of dense tensor-valued fields, for visualization purposes. Within the framework of anisotropic diffusion PDE's, we focus on the general trace-based expressions (that we previously investigated in [39]) that are particularly well adapted to control the local smoothing performed by the regularization processes. Using this formalism, we propose then a new PDE which uses the spectral informations of a tensor field $\mathbf{T} : \Omega \to \mathcal{P}_n$ to a create texture view of $\mathbf{T}$, starting from an image of pure noise. We show moreover how our method can be practically applied, using a precise numerical scheme based on local filtering considerations. The equation is then considered to deal specifically with DT-MRI datasets (Diffusion Tensor-MRI), offering an alternative solution to parametric methods for the visualization of fibers bundles in the biological tissues. Application results are finally proposed with the visualization of fibers within the white matter of the brain.

1 Introduction

Since the pioneering work of Perona-Malik [23], anisotropic regularization PDE's raised a strong interest in the field of image processing. The benefit of PDE-based regularization methods lies in the ability to smooth data in a nonlinear way, allowing the preservation of important image features (contours, corners or other discontinuities). Thus, many regularization schemes have been presented so far in the literature, particularly for the problem of scalar image restoration ([3, 12, 10, 12, 22, 26, 27, 44] and references therein). Recent extensions of these schemes to vector-valued images $\mathbf{I} : \Omega \to \mathbb{R}^n$ have been also considered, leading to diffusion PDE's with additional coupling terms between image channels ([7, 16, 28, 31, 35, 37, 39, 41, 44]).

Despite this wide range of existing regularization PDE formalisms, the methods have something in common : The idea is to locally smooth the image data along one or two particular directions that are different for each image point (typically, the principal smoothing direction is orthogonal to the image discontinuities). It results then in an anisotropic smoothing process. The way this local diffusion behavior is defined is not unique and different formalisms have been already considered in the literature for that purpose.

Basically, one wants to separate the diffusion process itself and its underlying *diffusion structure*, i.e the geometry of the local smoothing performed by the PDE, that is the definition of smoothing directions and intensities on each image point. Methods to do that were proposed for instance in [42, 44], with a diffusion equation such as $\frac{\partial I}{\partial t} = \mathrm{div}\,(\mathbf{D}\nabla I)$ (where the tensor field $\mathbf{D} : \Omega \to \mathrm{P}_n$ represents the desired local regularization behavior), and more recently in [39, 34], where we rather proposed to use a trace-based PDE $\frac{\partial I}{\partial t} = \mathrm{trace}\,(\mathbf{DH})$ to perform such local smoothing.

In this paper, we propose to extend our last work [39] for the particular problem of tensor field visualization, and we design a specific diffusion PDE that creates a textured image from a general tensor field $\mathbf{T} : \Omega \to \mathcal{P}_n$ (denominated as a *flow*, $n = 2$ or 3), starting from a noisy image $I_{(t=0)}$. The visualization of vector fields $\mathbf{u} : \Omega \to \mathbb{R}^n$ will be also considered, as a particular case of tensor field visualization, with $\mathbf{T} = \mathbf{u}\mathbf{u}^T$ (illustration on Fig.1).

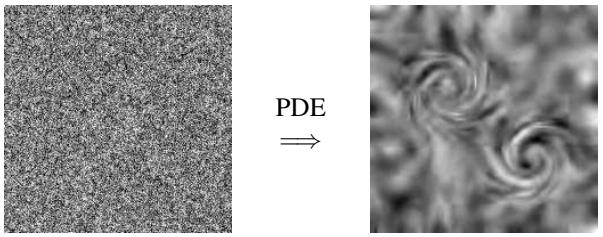

(a) Image $I_{(t=0)}$ at $t = 0$ (b) Image $I_{(t)}$ at $t = \alpha > 0$

Figure 1: *Creation of a textured Image from a Flow* $\mathbf{T} : \Omega \to \mathcal{P}_2$.

A similar formalism has been proposed in [5, 25] for $2D$ vector field visualization, based on a divergence equation such as $\frac{\partial I}{\partial t} = \mathrm{div}\,(\mathbf{D}\nabla I)$, where $\mathbf{D}$ is constructed from the vector field.

Our method is somehow different. By reviewing the wide range of existing PDE-based regularization formalisms, we first show that divergence-based equations are not always adapted to define precisely the local smoothing structure of

a regularization process. We rather focus on an alternative formulation expressed through a *trace-based PDE* that has a simple interpretation in terms of local filtering, done with adjusting gaussian kernels (section 2). Then, we investigate this formalism and extend it to deal with the visualization of $2D$ or $3D$ orientation or tensor fields. Differences with the approach proposed in [5, 25] will be discussed.

The particular interest of this new formalism is the use of a specific numerical scheme that is naturally associated with the proposed trace-based PDE, and which can be implemented with *local convolution* operators. In one hand, this makes a link between a general class of PDE expressions and existing adaptive filtering techniques such as Bilateral Filtering [4, 33] and more recently Short Time Kernel [30]. In the other hand, this new numerical scheme improves the obtained visualization results since it avoids the computation of second order derivatives that are needed for classical regularization schemes.

Our PDE approach can be used for the visualization of any tensor or vector field. Thus, we specialize it for the particular case of DT-MRI fiber visualization (section 3). Diffusion-Tensor MRI is a recent and non-invasive 3D medical modality that measures the motion of water molecules within biological tissue fibers. This is particularly helpful to retrieve fiber bundles and study the connectivity of the neurons through the white matter of the brain. We illustrate how our proposed flow visualization algorithm can be successfully used to create dense representations of these fibers networks from DT-MRI dataset of the brain (section 4).

2 A Local Analysis of Regularization PDE's

2.1 Existing regularization formalisms

In this section, we do a brief summary of our recent statements proposed in [39, 34], about classical regularization formalisms based on PDE's and variational tools, applying for $2D$ scalar images $I : \Omega \to \mathbb{R}$ (extensions to $3D$ volumes are generally straightforward). We particularly emphasize the behaviors of the equations in terms of local smoothing. Despite the huge literature on regularization PDE's ([3, 7, 10, 12, 16, 22, 31, 28, 27, 29, 32, 35, 38, 37, 39, 41, 44] among others), proposed regularization schemes are generally complying with one of these standpoints :

(1) Functional minimization : Regularizing an image I may be seen as the minimization of a functional $E(I)$ measuring a *global* image variation :

$$\min_{I:\Omega\to\mathbb{R}^n} E(I) = \int_\Omega \phi(\|\nabla I\|)\, d\Omega \qquad (1)$$

where $\phi : \mathbb{R} \to \mathbb{R}$ is an increasing function and the gradient norm $\|\nabla I\| = \sqrt{I_x^2 + I_y^2}$ is directly related to the local variations of the image I [12]. The computation of the Euler-Lagrange equations of (1) gives the corresponding divergence-based PDE that minimizes $E(I)$:

$$\frac{\partial I}{\partial t} = \mathrm{div}\,(\mathbf{D}\nabla I) \quad \text{with} \quad \mathbf{D} = \frac{\phi'(\|\nabla I\|)}{\|\nabla I\|}\,\mathbf{Id} \qquad (2)$$

where $\mathbf{Id}$ denotes the identity matrix.

Despite the global formulation of these regularization functionals (1), one can easily found the corresponding PDE (2) that is representative of the local smoothing performed by the minimization process, in the form of a *divergence expression*. These equations fit then the following framework.

(2) Divergence expressions : Some authors also proposed to design regularization PDE's directly from a local viewpoint, as the diffusion of pixel values,viewed as chemical concentrations [15, 44] and driven by a *field of diffusion tensors* $\mathbf{D} : \Omega \to \mathcal{P}_2$ (symmetric and positive matrices) :

$$\frac{\partial I}{\partial t} = \mathrm{div}\,(\mathbf{D}\nabla I) \quad \text{where} \quad \forall (x,y) \in \Omega, \qquad (3)$$

$$\mathbf{D}_{(x,y)} = \lambda_{1_{(x,y)}}\,\mathbf{u}_{(x,y)}\mathbf{u}_{(x,y)}^T + \lambda_{2_{(x,y)}}\,\mathbf{v}_{(x,y)}\mathbf{v}_{(x,y)}^T$$

In [15, 44], it has been assumed that the orthogonal eigenvectors $\mathbf{u}$,$\mathbf{v}$ and the positive eigenvalues λ_1,λ_2 of $\mathbf{D}$ give the two weights and directions of the local smoothing simultaneously performed by the PDE (3). $\mathbf{D}$ is then usually designed from the spectral elements of the gaussian blurred structure tensor $\mathbf{J}_\sigma = (\sum_i \nabla I \nabla I^T) * G_\sigma$ [14, 19, 43], in order to smooth I anisotropically, while respecting its discontinuities. Anyway, this interpretation of $\mathbf{D}$ as tensors giving the local smoothing geometry of (3) should not be systematic :

Indeed, the fact that the divergence $\mathrm{div}\,(..)$ is a *differential operator* necessary introduces the notion of a variation $\partial\mathbf{D}$ of the diffusion tensor field $\mathbf{D}$. Then, one cannot neglect the influence of the spatial variations $\frac{\partial \mathbf{D}}{\partial x}$ and $\frac{\partial \mathbf{D}}{\partial y}$ of $\mathbf{D}$, for understanding the effective smoothing performed by the diffusion PDE (3). It particularly means that if the chosen tensor field $\mathbf{D}$ has high variations (which is usual since $\mathbf{D}$ is generally constructed for preserving image discontinuities), nothing prevents the diffusion process (3) to smooth locally the image I with directions and intensities *that are different than those given pointwise by the spectral elements of the tensor* $\mathbf{D}(x,y)$. It can be more precisely understood as follows. The PDE (3) can be decomposed as :

$$\mathrm{div}\,(\mathbf{D}\nabla I) = \mathrm{trace}\,(\mathbf{D}\mathbf{H}) + \nabla I \,.\, \vec{\mathrm{div}}(\mathbf{D}) \qquad (4)$$

where $\mathbf{H} = \begin{pmatrix} \frac{\partial^2 I}{\partial x^2} & \frac{\partial^2 I}{\partial x \partial y} \\ \frac{\partial^2 I}{\partial x \partial y} & \frac{\partial^2 I}{\partial y^2} \end{pmatrix}$ is the Hessian matrix of I, and $\vec{\mathrm{div}}$ stands for the following differential operator, acting on matrices and returning vectors :

$$\text{if } \mathbf{D} = (d_{ij}), \qquad \vec{\mathbf{div}}\,(\mathbf{D}) = \begin{pmatrix} \mathrm{div}\,\left((d_{11} \;\; d_{12})^T\right) \\ \mathrm{div}\,\left((d_{21} \;\; d_{22})^T\right) \end{pmatrix}$$

The decomposition (4) simply separates the original divergence equation $\mathrm{div}\,(\mathbf{D}\nabla I)$ into two items :

• A regularization term $\mathrm{trace}\,(\mathbf{DH})$ that *does not depend* on the variation of the tensor field $\mathbf{D}$ (since $\mathrm{trace}\,(..)$ *is not* a differential operator). We will point out the fact that this trace-based equation is the one that smoothes effectively I using the geometric structure of the tensor $\mathbf{D}_{(x,y)}$ for each point $(x, y) \in \Omega$ of the image I.
• An additional term $\nabla I \,.\, \vec{\mathrm{div}}(\mathbf{D})$ that depends on the tensor field variation. This additional term may be disregarded on regions of Ω where the variations of the tensor field $\mathbf{D}$ are low (since then $\vec{\mathrm{div}}(\mathbf{D}) \simeq 0$), but *not in the general case*.

The well-known TV-regularization method [26] illustrates this fact. This widely used anisotropic diffusion PDE comes from the minimization of the functional :

$$\min \int_\Omega \|\nabla I\| \, d\Omega \implies \frac{\partial I}{\partial t} = \mathrm{div}\left(\frac{\nabla I}{\|\nabla I\|}\right) \qquad (5)$$

This is then equivalent to apply a divergence PDE such as $\frac{\partial I}{\partial t} = \mathrm{div}\,(\mathbf{D}\nabla I)$ with *isotropic tensors* $\mathbf{D} = \frac{1}{\|\nabla I\|}\,\mathbf{Id}$. These tensors have a double eigenvalue $\lambda_\pm = 1/\|\nabla I\|$ that is spatially varying over the definition domain Ω. Fortunately, the PDE (5) *does not perform locally an isotropic smoothing* despite the isotropic shape of the underlying tensors $\mathbf{D}$. Note that conversely, the first trace-based term acts indeed as a weighted Laplacian regularization (isotropic) $\frac{\partial I}{\partial t} = \mathrm{trace}\,(\mathbf{DH}) = \Delta I/\|\nabla I\|$ (Fig.2).

(a) Original noisy image (b) $\frac{\partial I}{\partial t} = \mathrm{div}\,(\mathbf{D}\nabla I)$. (c) $\frac{\partial I}{\partial t} = \mathrm{trace}\,(\mathbf{DH})$.

Figure 2: *Trace-based PDE's follow exactly the geometry of the tensors* $\mathbf{D} = \mathbf{Id}/\|\nabla I\|$.

The reason is that the second term $\nabla I \,.\, \vec{\mathrm{div}}(\mathbf{D})$ can be also written as :

$$\nabla I \,.\, \vec{\mathrm{div}}\left(\frac{1}{\|\nabla I\|}\,\mathbf{Id}\right) = \mathrm{trace}\left(-\frac{\nabla I \nabla I^T}{\|\nabla I\|^3}\mathbf{H}\right)$$

which corresponds to an *inverse diffusion along the gradient direction* (∇I is the main eigenvector of the tensor $-\nabla I \nabla I^T/\|\nabla I\|^3$). As a result the TV equation (5) can be also written as,

$$\frac{\partial I}{\partial t} = \mathrm{trace}\,(\mathbf{TH}) \quad \text{with} \quad \mathbf{T} = \frac{\nabla I^\perp \nabla I^{\perp T}}{\|\nabla I\|^3}$$

which means that the effective local smoothing would rather follow the geometry of a trace tensor $\mathbf{T}$ (with $\mathbf{T} \neq \mathbf{D}$), which is clearly anisotropic and always directed along the image contours $\nabla I^\perp$.

(3) Oriented Laplacians : Actually, this concept of trace-based PDE expression has been already proposed in another form by few authors. Indeed, a trace-based (6) can be also seen as the juxtaposition of *oriented 1D heat flows*, i.e mono-dimensional gaussian smoothing along orthonormal directions $\mathbf{u}\perp\mathbf{v}$, with corresponding weights c_1 and c_2 [17, 18, 28, 35, 37] :

$$\frac{\partial I}{\partial t} = c_1\,\frac{\partial^2 I}{\partial \mathbf{u}^2} + c_2\,\frac{\partial^2 I}{\partial \mathbf{v}^2} = \mathrm{trace}\,(\mathbf{TH}) \qquad (6)$$

where $\mathbf{H}$ is the Hessian matrix of I, c_1,c_2 and $\mathbf{u}$,$\mathbf{v}$ are respectively the positive eigenvalues and orthogonal eigenvectors of the tensors $\mathbf{T} = c_1\mathbf{u}\mathbf{u}^T + c_2\mathbf{v}\mathbf{v}^T$. This is actually a good way of designing regularization processes with desired local smoothing properties. Moreover, we will show now that this particular form of PDE's has a simple interpretation in terms of local filtering.

2.2 Trace-based PDE's and local convolutions

Let us first consider that the trace tensor $\mathbf{T}$ is constant over the definition domain Ω, in the PDE (6). Then, it can be shown [34, 39] that the formal solution of the PDE (6) is :

$$I_{(t)} = I_{(t=0)} \;*\; G^{(\mathbf{T},t)} \qquad (7)$$

where $*$ stands for the convolution operator and $G^{(\mathbf{T},t)}$ is an *oriented gaussian kernel*, defined by :

$$G^{(\mathbf{T},t)}(\mathbf{x}) = \frac{1}{4\pi t}\exp\left(-\frac{\mathbf{x}^T\mathbf{T}^{-1}\mathbf{x}}{4t}\right) \quad \text{with} \quad \mathbf{x} = (x \quad y)^T$$

Note that in this case, the divergence and trace-based expressions are equivalent : $\mathrm{div}\,(\mathbf{T}\nabla I) = \mathrm{trace}\,(\mathbf{TH})$.

When $\mathbf{T}$ is not constant (which is generally the case), i.e. represents a field $\Omega \rightarrow \mathrm{P}_2$ of varying diffusion tensors, the PDE (6) becomes *nonlinear* and can be viewed as the application of spatially varying *local masks* $G^{\mathbf{T},t}(\mathbf{x})$ over the image $\mathbf{I}$. This is not the case for divergence-based expressions, since an additional term $\nabla I \,.\, \vec{\mathrm{div}}(\mathbf{D})$ related to the *tensor field variation* appears, prohibiting the interpretation of the tensors as pointwise indicators of the regularization performed by the PDE process (3). This kind of term could be rather be seen as a *transport term* $\beta \,.\, \nabla I$.

This local filtering concept makes the link between a generic form of trace-based PDE's (6) and *Bilateral filtering* techniques [4, 33] or more recently Short Time Kernels [30], which are both based on local filtering considerations (with non-gaussian kernels for the STK).

The PDE (6) can be implemented with classical numerical schemes, based on centered spatial discretizations of the gradients and the Hessians [20]. But it is also possible to use the local filtering interpretation of the equation with this alternative approach : As the equation is equivalent to perform local convolutions with oriented gaussian kernels, the following scheme applies naturally for the the implementation of (6) :

$$\forall (x,y) \in \Omega, \quad I^{[t+1]} = \sum_{k,l=-l/2}^{l/2} \mathbf{G}^{(\mathbf{T},dt)}(k,l)\; I^{[t]}(x-k, y-l)$$

where dt represents the time step and l is a user-defined parameter that represents the size in pixels of the used gaussian kernels. The more l is large, the more precise the numerical approximation will be (Fig.6).

Main advantages of this numerical scheme are :

• At a current image point, more than just adjacent pixels are considered for the evolution of the PDE (if $l > 3$).

• The *maximum principle* is preserved, since the local filtering is done only with *normalized gaussian kernels*.

• It is more precise, since the computed kernels $\mathbf{G}^{(\mathbf{T},t)}$ do not depends on derivatives of the image I. For the particular case of image restoration, $\mathbf{G}$ depends only on the first derivative (gradient) or I, which leads to better numerical approximations of the PDE. Moreover, for our proposed flow visualization technique (section 3), no images derivatives have to be computed, since the tensor field $\mathbf{T}$ will even not depend on the structure tensor.

As for shortcomings, we have to mention that it is specially time-consuming, since it needs the computation of several gaussian masks (i.e. exponentials functions) for each image point and each PDE iteration.

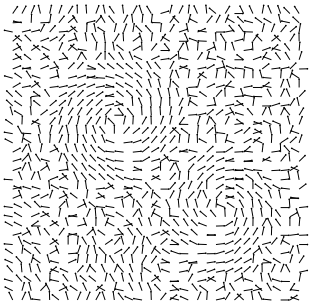

(a) Flow visualization with arrows

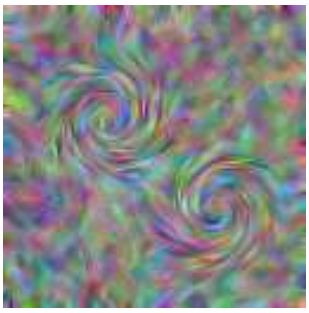

(b) Flow visualization with PDE (8) (5 iter.)

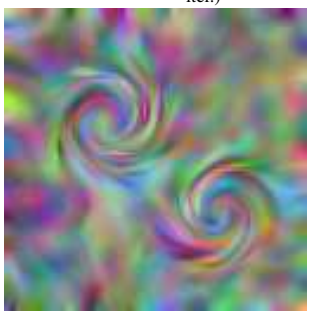

(c) Flow visualization with PDE (8) (15 iter.)

Figure 3: *Using regularization PDE (8), for 2D vector flow visualization.*

3 Flow visualization with PDE's

3.1 Principle of the method

Considering a 2D vector field $\mathcal{F} : \Omega \to \mathbb{R}^2$, we have several ways to visualize it. We can first use vectorial graphics, but we have to subsample the field since this kind of representation is not adapted to represent big flows. A better solution is as follows. Starting from a completely noisy image $\mathbf{I}$, we apply this trace-based regularizing PDE that smoothes the image *exactly in the directions of the vectors* :

$$\frac{\partial I}{\partial t} = \text{trace}\left(\left[\frac{1}{\|\mathcal{F}\|}\mathcal{F}\mathcal{F}^T\right]\mathbf{H}\right) \qquad (i = 1..n) \qquad (8)$$

This equation creates a textured image that represents the different structures of the flow $\mathcal{F}$, thanks to its highly anisotropic behavior.

Whereas the PDE evolution time t goes by, more global structures of the flow $\mathcal{F}$ appear, i.e. a visualization *scale-space* of $\mathcal{F}$ is constructed (Fig.3). Here, our used regularization equation (8) *ensures that the smoothing of the pixels is done exactly in the direction of the flow* $\mathcal{F}$. This is not the case in [5, 8, 13], where the authors based their equations on divergence expressions. Using similar divergence-based techniques would raise a risk of smoothing the image in false directions, as this has been pointed out above.

3.2 Extension to DT-MRI

Diffusion-Tensor MRI is a technique allowing the measurement of the *water molecule motion* in the tissues fibers, by the mean of rendering multiple MRI images under different oriented magnetic fields. This large set of raw data is then further estimated into a *volume of 3D diffusion tensors* $\mathbf{T}$: $\Omega \subset \mathbb{R}^3 \to \mathrm{P}(3)$ (i.e. 3×3 symmetric and positive-definite matrices) that describe through their spectral elements, the main diffusivities $\lambda_1, \lambda_2, \lambda_3$ (with $\lambda_1 \geq \lambda_2 \geq \lambda_3$) and the corresponding principal orthogonal directions $\mathbf{u}^{[1]}$,$\mathbf{u}^{[2]}$,$\mathbf{u}^{[3]}$ of the water molecule diffusion in tissues such as bones, muscles and white matter of the brain (Fig.4b).

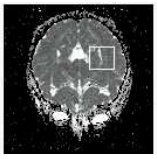

(b1) Mean diffusivity = $\frac{1}{3}(\lambda_1 + \lambda_2 + \lambda_3)$

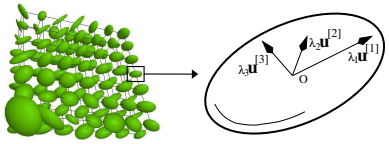

(b2) Part of the estimated tensor field $\mathbf{T}$, represented with 3D ellipsoids.

Figure 4: *Volumes of Diffusion-Tensor MRI.*

DT-MRI images are well suited to study the fiber network in the white matter of the brain. The need to visualize such fibers bundles has recently raised a strong interest for specific visualization techniques dedicated to this issue (very close to the ones encountered in flow visualization, in the domain of applied physics). Common visualization methods for DT-MRI images are :

• **Ellipsoids** are the natural representations of diffusion tensors. They are well adapted to see independently each DT-MRI voxel, and its spectral elements. Nevertheless, they are not suitable to display large fields of DT-MRI because of the high number of ellipsoids needed : as illustrated on Fig.7a (left), displaying large tensor fields with ellipsoids can be confusing.

• **Streamlines** are parametric representations of the fibers. They are constructed from the tensor field by drawing

lines following the diffusion tensor principal orientations $\mathbf{u}$. Well adapted for displaying fibers of medium-size parts of the tensor field, they can also be confusing for larger ranges of view Fig.7a (right).

• **LIC** (line integral convolution). As proposed in [9, 21], the idea is to integrate a noise texture in the direction of the principal tensor direction, leading to a texture-representation of the flow. It is more adapted to display fibers in larger DT-MRI regions, but is more time-consuming.

3.3 Proposed method

We propose here an alternative method to visualize a $3D$ diffusion tensor field $\mathbf{T} : \Omega \rightarrow \mathcal{P}_3$, based on regularization PDE's. The idea is as follows. Starting from a noisy 3D volume $I_0 : \tilde{\Omega} \rightarrow \mathbb{R}$ (uniform noise), we apply this specific PDE flow :

$$\left\{ \begin{array}{rcl} I_{(t=0)} & = & I_0 \\ \\ \dfrac{\partial I}{\partial t} & = & \mathrm{trace}\,(\mathbf{DH}) \end{array} \right. \quad (9)$$

where $\mathbf{D} : \Omega \rightarrow \mathrm{P}(3)$ is another diffusion tensor field computed from $\mathbf{T}$ as :

$$\forall x, y, z, \qquad \mathbf{D} = \mathbf{u}\mathbf{u}^T + g(FA)\ (\mathbf{Id} - \mathbf{u}\mathbf{u}^T)$$

where $\mathbf{u}$ is the principal direction of $\mathbf{T}$, $\mathbf{Id}$ is the identity matrix and $g : [0,1] \rightarrow [0,1]$ is a decreasing function. The Fractional Anisotropy FA is defined as :

$$FA = \sqrt{\frac{(\lambda_1-\lambda_2)^2+(\lambda_1-\lambda_3)^2+(\lambda_2-\lambda_3)^2}{2(\lambda_1^2+\lambda_2^2+\lambda_3^2)}}$$

Its value characterizes the shape of a tensor (isotropic for low values, and anisotropic for high values) [24]. We do not choose directly $\mathbf{D} = \mathbf{T}$ since it could quickly oversmoothes the noisy image I. Moreover, our proposed equation (9) has the interesting property of smoothing the image I in the principal directions of the tensors where they are anisotropic (i.e. $FA(x,y,z) >> 0$), while performing an isotropic smoothing where tensors are isotropic (i.e. $FA(x,y,z) \simeq 0$). This trace-based equation has a real interpretation in terms of local smoothing, and can be implemented using local convolution techniques, as described in section (2). Instead of the method proposed in [5, 25], we ensure here that the smoothing of the noisy image is done along the fiber directions, thanks to our trace-based PDE expression. Once the textured image has been obtained, we multiply it by the image of the Fractional Anisotropy FA :

$$I_{\text{final}} = I_{\text{regularized}} * FA$$

This allows to emphasize only regions of high anisotropy (i.e fibers), while attenuating regions of high isotropy (for instance the liquid in the CSF filled ventricles).

Our visualization technique is also well adapted to create multi-scale texture representations of the fiber structures in DT-MRI images. As illustrated in Fig.7,8, it is suited to view fibers in large portions of DT-MRI fields.

4 Experimental results

We illustrate the different aspects of our proposed visualization algorithm (9) on Fig.5,6,7 :

• Fig.5 shows the scale-space property of our method, inherent to the use of a regularization PDE technique. Starting from a noisy image, we create a textured representation of a flow $\mathcal{F}$ (here, a tensor field). Progressively, the noisy image is smoothed and thin details of the flow $\mathcal{F}$ softly disappear. It allows the representation of $\mathcal{F}$ at different scales, which are anisotropically computed by the PDE (9).

• Fig.6 illustrates the accuracy of our proposed numerical scheme (section 2.2), based on local convolutions with adjusting gaussian kernel. If we use a classical finite difference scheme to approximate the PDE term $\mathrm{trace}\,(\mathbf{TH})$, directions of the flow $\mathcal{F}$ that are not directed along the main axes X or Y may appear oversmoothed (Fig.6a). Conversely, the use of adjusting gaussian kernels to perform the diffusion avoid this effect until the size l of the convolution masks used is large enough (practically, $l >= 7$ pixels).

• Fig.7 and 8 are two results of fiber tracking in different regions of the corpus callosum, from DT-MRI datasets. This region located in the white matter of the brain is representative of the fiber bundles, since it links the two hemispheres of the brain. On the left, the DT-MRI data are displayed using ellipsoids and lines that represent tracked fibers (Fig.7a). On the right, fibers appear naturally by applying our flow-visualization technique (9) on a noisy 3D volume. As we may notice, this display mode is more perceptible for such dense DTMRI datasets.

Conclusion & Perspectives

We analyzed how regularization PDE's are performing local smoothing and used it to design a new diffusion PDE that creates textured images from general input flows. Our formulation allows the visualization of big portions of dense vector or tensor fields, and has been used to create fiber tracking results in the white matter of the brain, thanks to the use of DT-MRI datasets. The proposed numerical scheme has proven its efficiency beside classical finite difference schemes. The fast computation of the results is an open problem of interest, which we are working on.

References

[1] L. Alvarez, R. Deriche, J. Weickert, and J. Sànchez. Dense disparity map estimation respecting image discontinuities: A PDE and scale-space based approach. *International Journal of Visual Communication and Image Representation, Special Issue on Partial Differential Equations in Image Processing, Computer Vision and Computer Graphics*, 2000.

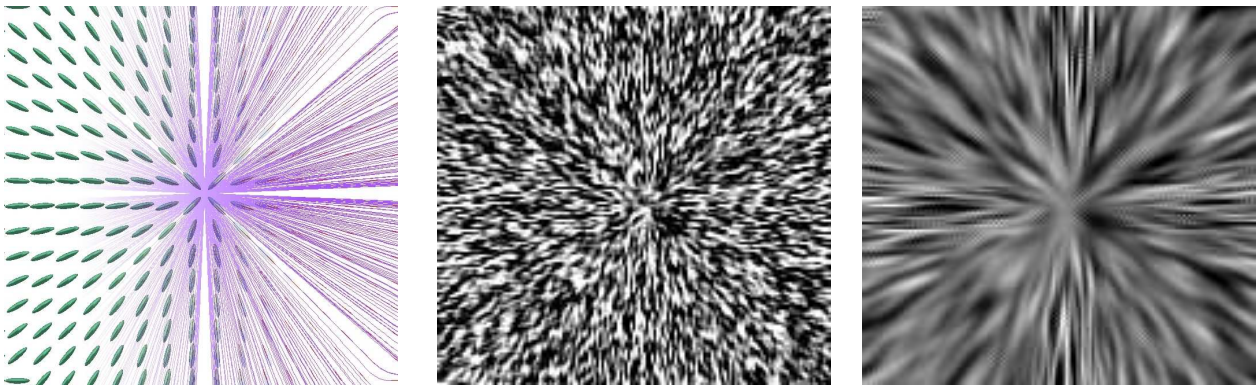

(a) Visualization of $\mathbf{T}$ with parametric ellipsoids/fibers (b) Using our visualization PDE (9) after 10 it. (c) Using our visualization PDE (9) after 30 it.

Figure 5: Constructing a scale-space visualization of a diffusion tensor field $\mathbf{T}$, with PDE (9).

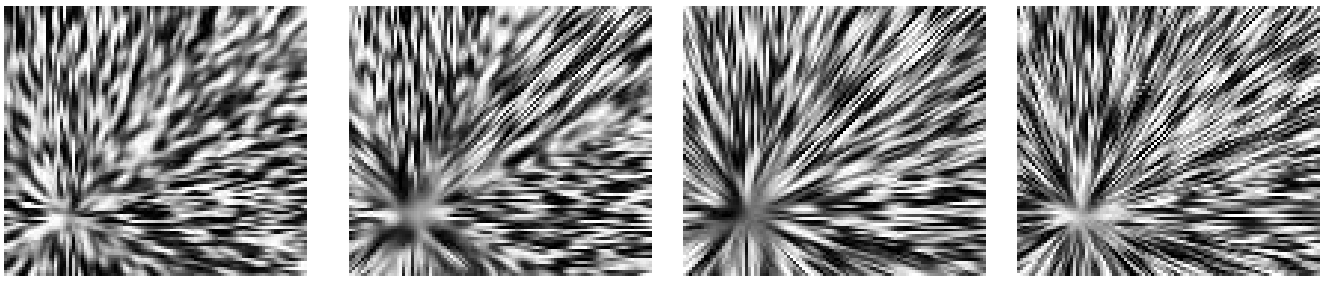

(a) Using a finite-difference scheme (27 it.) (b) Using 3x3 Gaussian kernels (9 it.) (c) Using 7x7 Gaussian kernels (3 it.) (d) Using 15x15 Gaussian kernels (2 it.)

Figure 6: Comparisons of numerical schemes for Flow Visualization.

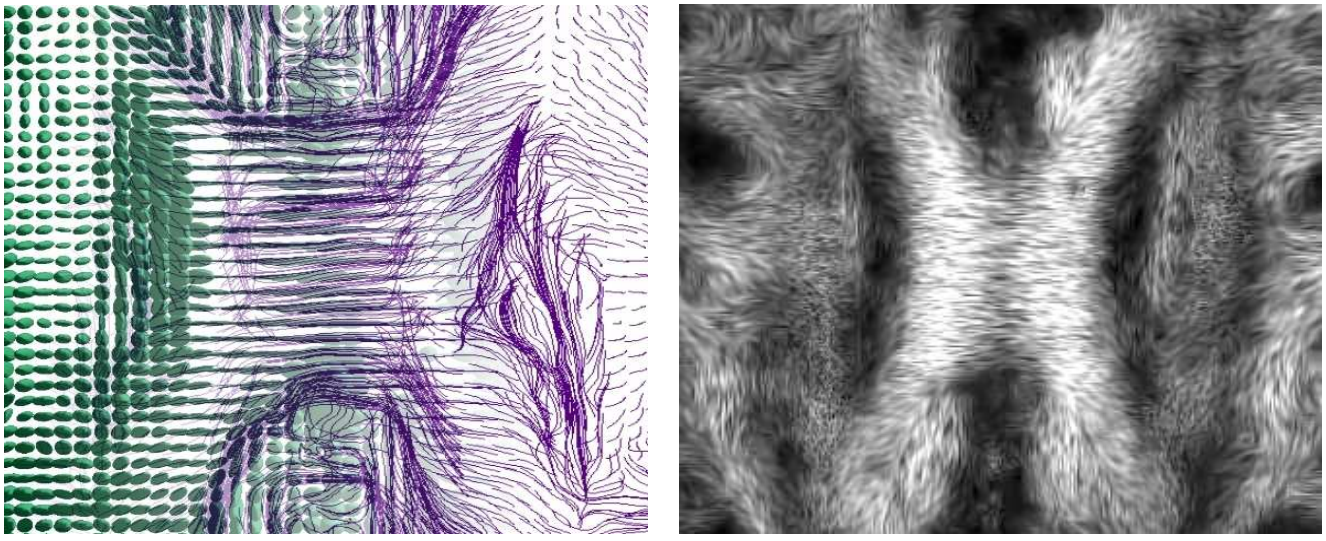

(a) Tensor field displayed with ellipsoids (left) and tracked fibers (right) (b) Fiber network, created using our PDE approach (9)

Figure 7: **DT-MRI Visualization** : Using Parametric(left) or PDE-based(right) visualization of the fiber bundles in a part of the Corpus Callosum.

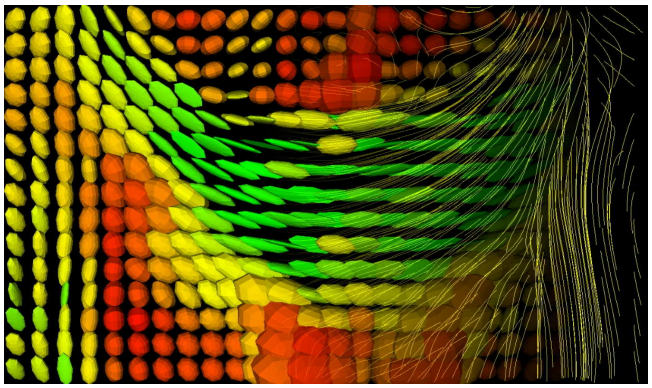

(a) Tensor field displayed with ellipsoids (left) and tracked fibers (right), and colored by Fractional Anisotropy FA.

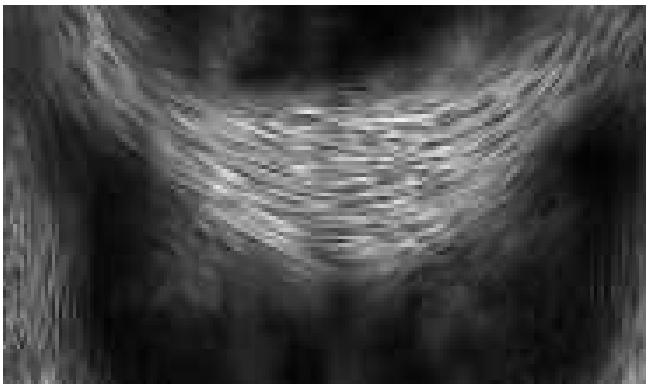

(b) Fiber network, created using our visualization PDE approach (9)

Figure 8: **DT-MRI Visualization (2)** : Using Parametric(left) or PDE-based(right) visualization of the fiber bundles in a part of the Corpus Callosum.

[2] Luis Alvarez. Images and PDE's. In M.O. Berger, R. Deriche, I. Herlin, J. Jaffre, and J.M. Morel, editors, *Images,Wavelets and PDEs*, volume 219 of *Lecture Notes in Control and Information Sciences*. Springer, June 1996.

[3] G. Aubert and P. Kornprobst. *Mathematical Problems in Image Processing: Partial Differential Equations and the Calculus of Variations*, volume 147 of *Applied Mathematical Sciences*. Springer-Verlag, January 2002.

[4] D. Barash. Bilateral filtering and anisotropic diffusion : Towards a unified viewpoint. Technical report, HP Laboratories Israel, 2000.

[5] J. Becker, T. Preusser, and M. Rumpf. Pde methods in flow simulation post processing. *Computing and Visualization in Science*, 3(3):159–167, 2000.

[6] M.J. Black, G. Sapiro, D.H. Marimont, and D. Heeger. Robust anisotropic diffusion. *IEEE Trans. Imag. Proc.*, 7(3):421–432, 1998. Special Issue on Partial Differential Equations and Geometry-Driven Diffusion in Image Processing and Analysis.

[7] P. Blomgren and T.F. Chan. Color tv: Total variation methods for restoration of vector-valued images. *IEEE Trans. Imag. Proc.*, 7(3):304–309, 1998. Special Issue on Partial Differential Equations and Geometry-Driven Diffusion in Image Processing and Analysis.

[8] D. Buerkle, T. Preusser, and M. Rumpf. Transport and diffusion in timedependent flow visualization. In *Proceedings IEEE Visualization*, 2001.

[9] B. Cabral. Imaging vector fields using line integral convolution. In *Computer Graphics Proceedings*, pages 263–270, 1993.

[10] A. Chambolle and P.L. Lions. Image recovery via total variation minimization and related problems. *Nümerische Mathematik*, 76(2):167–188, 1997.

[11] T. Chan and J. Shen. Variational restoration of non-flat image features : Models and algorithms. *Research Report. Computational and applied mathematics department of mathematics Los Angeles.*, June 1999.

[12] P. Charbonnier, L. Blanc-Féraud, G. Aubert, and M. Barlaud. Deterministic edge-preserving regularization in computed imaging. *IEEE Transactions on Image Processing*, 6(2):298–311, 1997.

[13] U. Diewald, T. Preusser, and M. Rumpf. Anisotropic diffusion in vector field visualization on euclidian domains and surfaces. *IEEE Transactions on Visualization and Computer Graphics*, 6(2):139–149, 2000.

[14] M. A. Förstner and E. Gülch. A fast operator for detection and precise location of distinct points, corners and centers of circular features. In *Proceedings of the Intercommission Workshop of the International Society for Photogrammetry and Remote Sensing*, Interlaken, Switzerland, 1987.

[15] G. Gerig, O. Kubler, R. Kikinis, and F. Jolesz. Nonlinear anisotropic filtering of mri data. *IEEE TMI*, 11(2):221–231, 1992.

[16] R. Kimmel, R. Malladi, and N. Sochen. Images as embedded maps and minimal surfaces: movies, color, texture, and volumetric medical images. *International Journal of Computer Vision*, 39(2):111–129, September 2000.

[17] P. Kornprobst, R. Deriche, and G. Aubert. Nonlinear operators in image restoration. In *Proceedings of the International Conference on Computer Vision and Pattern Recognition*, pages 325–331, Puerto Rico, June 1997. IEEE Computer Society, IEEE.

[18] Karl Krissian, Grégoire Malandain, and Nicholas Ayache. Directional anisotropic diffusion applied to segmentation of vessels in 3d images. Technical Report 3064, INRIA, December 1996.

[19] Tony. Lindeberg. *Scale-Space Theory in Computer Vision*. Kluwer Academic Publishers, 1994.

[20] Laurence Lucido, Rachid Deriche, Luis Alvarez, and Vincent Rigaud. Sur quelques schémas numériques de résolution d'équations aux dérivées partielles pour le traitement d'images. Rapport de Recherche 3192, INRIA, June 1997.

[21] T.E. McGraw. Neuronal fiber tracking in dt-mri. Master's thesis, University of Florida, 2002.

[22] J.M. Morel and S. Solimini. Segmentation of images by variational methods: A constructive approach. *Rev. Math. Univ. Complut. Madrid*, 1:169–182, 1988.

[23] P. Perona and J. Malik. Scale-space and edge detection using anisotropic diffusion. *IEEE Transactions on Pattern Analysis and Machine Intelligence*, 12(7):629–639, July 1990.

[24] C. Poupon. *Détection des faisceaux de fibres de la substance blanche pour l'étude de la connectivité anatomique cérébrale.* PhD thesis, Ecole Nationale Supérieure des Télécommunications, December 1999.

[25] T. Preusser and M. Rumpf. Anisotropic nonlinear diffusion in flow visualization. In *In Proceedings IEEE Visualization '01*, 2001.

[26] L. Rudin, S. Osher, and E. Fatemi. Nonlinear total variation based noise removal algorithms. *Physica D*, 60:259–268, 1992.

[27] G. Sapiro. *Geometric Partial Differential Equations and Image Analysis*. Cambridge University Press, 2001.

[28] G. Sapiro and D.L. Ringach. Anisotropic diffusion of multivalued images with applications to color filtering. *IEEE Transactions on Image Processing*, 5(11):1582–1585, 1996.

[29] J. Shah. Curve evolution and segmentation functionals: Applications to color images. In *Proceedings of the International Conference on Image Processing*, pages 461–464, 1996.

[30] N. Sochen, R. Kimmel, and A.M. Bruckstein. Diffusions and confusions in signal and image processing. *Journal of Mathematical Imaging and Vision*, 14(3):195–209, 2001.

[31] N. Sochen, R. Kimmel, and R. Malladi. A geometrical framework for low level vision. *IEEE Transaction on Image Processing, Special Issue on PDE based Image Processing*, 7(3):310–318, 1998.

[32] B. Tang, G. Sapiro, and V. Caselles. Diffusion of general data on non-flat manifolds via harmonic maps theory : The direction diffusion case. *The International Journal of Computer Vision*, 36(2):149–161, February 2000.

[33] C. Tomasi and R. Manduchi. Bilateral filtering for gray and color images. In *Proceedings of the IEEE International Conference on Computer Vision*, pages 839–846, January 1998.

[34] D. Tschumperlé. *PDE's Based Regularization of Multivalued Images and Applications*. PhD thesis, Université de Nice-Sophia Antipolis, December 2002.

[35] D. Tschumperlé and R. Deriche. Constrained and unconstrained PDE's for vector image restoration. In Ivar Austvoll, editor, *Proceedings of the 10th Scandinavian Conference on Image Analysis*, pages 153–160, Bergen, Norway, June 2001.

[36] D. Tschumperlé and R. Deriche. Diffusion tensor regularization with constraints preservation. In *IEEE Computer Society Conference on Computer Vision and Pattern Recognition*, Kauai Marriott, Hawaii, December 2001.

[37] D. Tschumperlé and R. Deriche. Diffusion PDE's on Vector-Valued images. *IEEE Signal Processing Magazine*, 19(5):16–25, 2002.

[38] D. Tschumperlé and R. Deriche. Régularisation par EDP de champs de vecteurs orthonormés et applications. In *13ème Congrès RFIA'02*, Angers, January 2002.

[39] D. Tschumperlé and R. Deriche. Vector-valued image regularization with PDE's : A common framework for different applications. In *IEEE Conference on Computer Vision and Pattern Recognition*, Madison, Wisconsin (United States), June 2003.

[40] B. Vemuri, Y. Chen, M. Rao, T. McGraw, T. Mareci, and Z. Wang. Fiber tract mapping from diffusion tensor mri. In *1st IEEE Workshop on Variational and Level Set Methods in Computer Vision (VLSM'01)*, July 2001.

[41] J. Weickert. *Anisotropic Diffusion in Image Processing*. PhD thesis, University of Kaiserslautern, Germany, Laboratory of Technomathematics, January 1996.

[42] J. Weickert. Coherence-enhancing diffusion of colour images. *7th National Symposium on Pattern Recognition and Image Analysis*, April 1997.

[43] J. Weickert. A review of nonlinear diffusion filtering. *Scale-Space Theory in Computer Vision, Lecture Notes in Comp. Science (Springer, Berlin)*, 1252:3–28, 1997. Invited Paper.

[44] J. Weickert. *Anisotropic Diffusion in Image Processing*. Teubner-Verlag, Stuttgart, 1998.